Hybrid Communication Protocols and Control Algorithms for NextGen Aircraft Arrivals

Pangun Park, Harshad Khadilkar, Hamsa Balakrishnan, and Claire Tomlin

***Abstract*—Capacity constraints imposed by current air traffic management technologies and protocols could severely limit the performance of the Next Generation Air Transportation System (NextGen). A fundamental design decision in the development of this system is the level of decentralization that balances system safety and efficiency. A new surveillance technology called Automatic Dependent Surveillance-Broadcast (ADS-B) can potentially be used to shift air traffic control to a more distributed architecture; however, channel variations and interference with existing secondary radar replies can affect ADS-B systems. This paper presents a framework for managing arrivals at an airport using a hybrid centralized/distributed algorithm for communication and control. The algorithm combines centralized control in congested regions with distributed control in lower traffic density regions. The hybrid algorithm is evaluated through realistic simulations of operations around a major airport. The proposed strategy is shown to significantly improve air traffic control performance under various operating conditions, by adapting to the underlying communication, navigation and surveillance systems. The performance of the proposed strategy is found to be comparable to fully centralized strategies, despite requiring significantly less ground infrastructure.**

***Index Terms*—Hybrid Communication and Control, Conflict Detection and Resolution, ADS-B, NextGen.**

I. Introduction

Safety and efficiency are the main objectives of the air transportation system. The airspace today is divided into sectors, each of which has an air traffic controller who is responsible for managing the traffic within it. Aircraft within a given sector are controlled centrally by the corresponding air traffic controller. A significant increase in air traffic demand is expected over the next decade, which has motivated efforts to modernize air transportation systems by leveraging improved navigation and communication technologies [1]. In the US, this future system is referred to as the Next Generation Air Transportation System (NextGen) [1].

In the most congested regions of the airspace, centralized control of air traffic (in which a single entity controls all aircraft and information flows) will result in the most efficient operations. However, such centralization is expensive to implement on a large scale, since it requires information from all aircraft to be relayed to the central facility, either through surveillance or by communication. This problem is exacerbated as traffic demand increases. By contrast, interactions among aircraft are rare in regions of low traffic density, and a distributed control strategy (in which an aircraft unilaterally resolves conflicts) may be nearly as efficient as a centralized one. In such scenarios, a distributed system consists of multiple aircraft that cooperate for the safety and efficiency of air traffic management.

The current system relies on ground-based radars to provide centralized surveillance. Ground radars are very large structures that are expensive to deploy and need significant amounts of maintenance [2]. Furthermore, these systems are subject to terrain blockage, and cannot provide coverage in areas where there is no line-of-sight. Instead of relying on expensive ground radar technologies, NextGen aircraft will have enhanced onboard sensing capabilities, and carry wireless communication platforms [3], [4]. Wireless communication systems can operate beyond the line-of-sight constraints of radar and vision solutions, and enable cooperative techniques. The above observations suggest that an efficient and cost-effective strategy would combine centralized control in congested regions with distributed control in low-density ones.

Automatic Dependent Surveillance-Broadcast (ADS-B) is a NextGen surveillance and communication technology in which aircraft broadcast onboard flight information via datalink to ground stations or equipped aircraft within range [3], [4]. The position and velocity data are obtained using onboard satellite navigation systems. New communication and control algorithms need to be developed in order to effectively leverage the potential of technologies such as ADS-B. They need to account for the limitations of the new technologies, as well as their interactions with legacy infrastructure. Minimal procedural modifications are desirable for easy implementation and large-scale deployment. The increased surveillance accuracy and reduced latency of ADS-B improve onboard situation awareness, and make distributed control a feasible option. However, since ADS-B uses the same bandwidth as the replies to Secondary Surveillance Radars (SSRs), high aircraft and SSR density near airports could degrade the performance of both systems [5]. Therefore, communication and control algorithms must adapt to varying interference and traffic levels in order to ensure efficient aircraft operations, while maintaining safety.

This paper presents a framework for determining the optimal level of airspace decentralization, considering both the communication and control components. We consider a region around a large urban airport and the arrival traffic to that airport. The objective is to reduce flight times while guaranteeing

Pangun Park and Claire Tomlin are with the Department of Electrical Engineering and Computer Science, University of California at Berkeley, Berkeley, CA, e-mail: {pgpark|tomlin}@eecs.berkeley.edu. Harshad Khadilkar and Hamsa Balakrishnan are with the Department of Aeronautics and Astronautics, Massachusetts Institute of Technology, Cambridge, MA, e-mail: {harshadk|hamsa}@mit.edu.

This work has been supported in part by NSF under CPS:ActionWebs (CNS-931843), by ONR under the HUNT (N0014-08-0696) and SMARTS (N00014-09-1-1051) MURIs and by grant N00014-12-1-0609, by AFOSR under the CHASE MURI (FA9550-10-1-0567).

safety under increased traffic levels. Since the arrival flows into busy airports are among the most congested elements of the airspace, efficiency gains in these regions will yield system-wide benefits. The main contributions of this paper are the following: (1) A centralized/distributed communication protocol to improve surveillance performance, (2) a centralized/distributed control algorithm to minimize flight times while meeting safety constraints, and (3) the performance evaluation of the proposed hybrid centralized/distributed strategy through simulations under various conditions.

The remainder of this paper is organized as follows: Section II summarizes related work from the communications and control literature. Section III describes the system architecture, including the communication and control components. Section IV presents a communication protocol that adapts based on the level of decentralization. Section V describes the proposed centralized and distributed control algorithms. In Section VI, the performance of the proposed strategy is evaluated under several realistic scenarios. Finally, Section VII summarizes the main results in the paper. For simplicity, SSRs are referred to merely as *radars* in the reminder of this paper.

II. Related Work

Relevant literature on communication protocols is first considered in Section II-A. Aircraft control algorithms, especially pertaining to conflict resolution, are discussed in Section II-B.

A. Communication Protocols

Cooperative conflict detection and resolution strategies require communication and coordination between the aircraft involved [6]. Ideally, decisions made by each aircraft are based on complete state information about the entire network. Therefore, the key components of surveillance system design are the transmit power and channel access control. This section describes related work from literature on cellular and wireless ad hoc networks, and the challenges involved in applying existing solutions to air traffic surveillance.

Transmit power control of the physical layer is a key aspect in the design of communication protocols. The objectives of power control are the mitigation of multiple access interference and the conservation of battery power, a valuable resource in cellular and ad hoc networks. Power control has been extensively studied in the context of cellular systems [7] and ad hoc networks [8]. Distributed iterative power control algorithms have been introduced for different systems and fast convergence results have been established [7], [8]. In [9], a heuristic broadcast incremental power algorithm determines the minimum power tree routed at the source node, that reaches all the other nodes in the network. In general, power control is a difficult problem for which no scalable solutions are known for wireless networks. Furthermore, it is worth noting that most power control algorithms require a separate feedback channel that enables receivers to send their Signal-to-Interference-plus-Noise-Ratio (SINR) measurements back to the transmitters. However, in the broadcast scenario, it is inefficient to send an explicit feedback message due to overhead, contention between receivers and node mobility. It is therefore difficult to adapt the cellular version of distributed power control for ADS-B. Furthermore, in contrast to other wireless networks, the relative energy consumption of the communication component is typically small in control systems.

The design of the channel access mechanism is also important in communication networks. Conflict-free access provides channel control by explicit scheduling transmissions, leading to better channel utilization and handling of priorities, and greater stability. The problem of scheduling conflict-free transmissions in time division multiple access multi-hop packet radio networks has received considerable attention in the context of broadcast [10]. The objective of this approach is to use the shortest frames possible in order to obtain high spatial reuse. However, the construction of a broadcasting schedule of minimum length in a radio network is known to be NP-hard [11]. In mobile networks, scheduling protocols may require constant updates dependent on rapid changes of topology. Many topology-dependent scheduling algorithms require a recomputation of transmission schedules for each topology change [12]. The efficiency and robustness is therefore vulnerable in a mobile environment. Even if the reassignment of schedules after each topology change is done in a distributed way, significant overhead is generated [12].

The contention access mechanism is characterized by its simplicity in terms of implementation, but it does not provide the nodes with deterministically guaranteed performance [13]. The fair allocation of bandwidth among different nodes is one of the critical problems that affects the stability and safety of the control system. Prior research focuses on the fairness issues of single-hop wireless networks [14], [15]. Recently, there has been considerable interest to study the fairness of multi-hop wireless networks [16], [17]. A centralized max-min fairness approach for wireless mesh networks which strives to achieve end-to-end fairness is presented in [16]. In [17], a centralized algorithm is presented for achieving lexicographic max-min fairness in wireless sensor networks. However these papers address the problem for fixed infrastructure based wireless access networks which is different from our scenario. Our aim is to present a distributed solution as compared to the centralized solution for mobile networks.

B. Air Traffic Control Strategies

The most unrestricted form of air traffic control is the free flight concept, as described in [18]. In this scenario, an optimal trajectory is calculated by each aircraft using current traffic information. A range of free-flight objectives has been considered in literature, including maximizing safety [19] and minimizing flight times [20]–[22]. Time-optimal trajectories are calculated using mixed-integer linear programming for a two-dimensional airspace model in [23] and similar three-dimensional ones in [20] and [22]. These studies typically solve small-scale versions of the problem, since optimization formulations for stochastic systems of realistic size quickly become computationally intractable [24]. For practical reasons, it is desirable to maintain the current airspace layout for operational implementation. In contrast to previous approaches, this paper relaxes the assumption that state information from all aircraft is continuously available.

Air traffic control algorithms can be broadly classified into two types, namely, centralized and distributed approaches. Distributed algorithms [21], [25], [26], [27] are typically based on negotiations among aircraft to find optimal conflict resolution maneuvers, or can be developed based on non-cooperative game theory. Free-flight approaches typically fall into this category of algorithms. By contrast, centralized algorithms [20], [22], [23], [28] assume that information is consolidated at a single central facility, which then solves for the optimal trajectories for all aircraft. Information gathering is usually via ground radar systems, although recent papers have considered the availability of ADS-B. An extensive overview of strategies for conflict resolution can be found in [6].

At very short time-scales, conflict resolution is performed by onboard collision avoidance systems, such as the Traffic Collision Avoidance System (TCAS) [29], [30], or the proposed Airborne Collision Avoidance System [31], [32]. The requirements of these systems are tailored for onboard collision avoidance, and not for long-range efficiency. Implementing conflict resolution over a long time-scale is known to yield more efficient trajectories [33]. However, onboard collision avoidance systems cannot easily be extended to long range conflict resolution due to their limited range (typically $14\,\mathrm{nm}$) and poor performance in high-density airspaces [30].

This paper proposes a hybrid centralized/distributed algorithm for conflict detection and resolution. It combines distributed control in low-density airspace, with centralized control in the high-density terminal areas. This hybrid approach offers the dual advantage of reduced ground infrastructure cost due to decentralization and the efficiency of centralization, by appropriately classifying regions of airspace for each type of control. The paper shows that the control strategy minimizes the time required to land all the aircraft currently present in the airspace being considered, if state measurements are accurate. It also shows that for the two-aircraft scenario, the stability of the control strategy is governed by a geometric constraint on the maximum time interval between state updates. Furthermore, to the best of the authors' knowledge, this paper is the first one that considers a detailed communication model for the surveillance network along with the control problem.

III. System Architecture

The system architecture proposed in this paper combines the communication and control components of air traffic management. Fig. 1 shows the airspace model, based on the Los Angeles International Airport (LAX) terminal-area or Terminal Radar Approach and Control (TRACON). The system is composed of a centralized control region for aircraft close to the airport and a distributed control region for aircraft farther out. The centralized zone is a circle of radius R, while outside it is a concentric disc around the centralized region. Designated intersections of two or more arrival paths in the airspace are known as fixes, while the straight-line paths between two fixes are called links.

In the centralized region, surveillance is conducted by ADS-B ground stations and radar systems. Ground stations receive state information about aircraft within range from their ADS-B transmissions. The radars scan through 360° of azimuth and

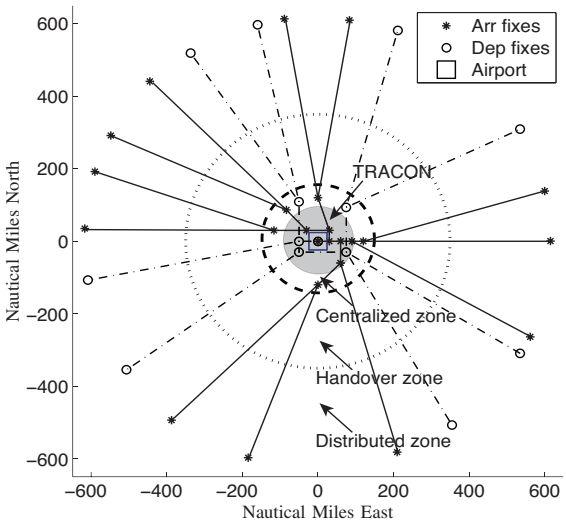

Fig. 1: TRACON layout modeled on LAX approach.

send information to central facilities [34]. Each radar interrogates aircraft transponders within range, which respond using a directional antenna. The interrogations are transmitted in the 1030 MHz band, and the replies are sent by aircraft in the 1090 MHz band. Since ADS-B operations share the 1090 MHz channel with radar replies, it uses a random access mechanism to avoid the interference of existing systems. The interference between the radar and ADS-B systems is investigated in [5]. In the ADS-B standard, each aircraft separately transmits the position and velocity messages at a rate of 2 messages per second [3]. The position or velocity information is inserted into the 56-bit message field using a 112-bit long ADS-B message. The transmit power is fixed between $51 - 57$ dBm. As the density of ADS-B avionics grows, increased interference levels could adversely affect the performance of both the radar and ADS-B systems [5]. It is important to ensure that the signals transmitted by ADS-B avionics do not degrade the sensing ability of the radars. Therefore, aircraft in the centralized zone use the minimum ADS-B transmit power and minimum channel access probability. The centralized control algorithm calculates the optimal velocities for all aircraft, based on their last known information.

Outside the centralized zone, the airspace is further divided into the handover and distributed zones. In the distributed zone, each aircraft uses an adaptive channel access algorithm to minimize the State Update Interval (SUI), that is, the time between its successful state vector reports. Maximum transmit power is used in this region in order to maximize information coverage. The channel access algorithm coordinates independent message transmissions to mitigate strong levels of interference, which cannot be overcome by power control alone. The handover zone is located between the centralized and distributed zones. Each aircraft adapts its transmit power while maintaining the default channel access probability. The details of the communication protocol are presented in Section IV. Distributed control uses only ADS-B surveillance, and is valid in both the handover and distributed zones. The proposed control algorithm is described in Section V.

IV. Communication Protocols

This section describes a distributed power control and channel access control of ADS-B. Given a transmit power, each aircraft transmits an ADS-B message with a given channel access probability. Each aircraft determines its transmit power and channel access probability by considering its information coverage, SUI, and interference with radars.

A. Power Control

An algorithm that determines the transmit power of ADS-B based on the distance of each aircraft from the centralized boundary is presented here. The goal is to tune the transmit power such that information coverage of each aircraft is maximized while limiting interference with radars. A wireless link is characterized by the condition for successful reception, defined as $\mathrm{SINR} \geq \beta$, where β is a predefined threshold [3]. It is assumed that b_i is the range up to which aircraft i intends to broadcast its messages. Given a noise ϵ and assuming zero interference, the optimal transmit power p_i for range b_i is

$$p_i = \beta \epsilon b_i^{\alpha},$$

where the path loss exponent α is a parameter that typically takes a value between 2 and 4 [35]. We assume an Additive White Gaussian Noise (AWGN) ϵ with a zero-mean and standard deviation σ. By considering the feasible range of the transmit power $[p_{\min}, p_{\max}]$, the power update relation for aircraft i is

$$p_i = \begin{cases} \max\left(p_{\min}, \min\left(p_{\max}, \beta \epsilon g_i^{\alpha}\right)\right) & \text{for } g_i \geq 0 \\ p_{\min} & \text{for } g_i < 0 \end{cases} \quad (1)$$

where g_i is the distance from aircraft i to the boundary of the centralized zone. When the aircraft is far away from the centralized zone, the maximum transmit power, $p_{\max}$, is used, which corresponds to the fully distributed zone. As the aircraft approaches the centralized zone, it decreases its transmit power in the handover zone to $\beta \epsilon g_i^{\alpha}$, in order to reduce the inference with the radars. Once inside the centralized zone ($g_i < 0$), each aircraft uses the minimum transmit power, $p_{\min}$.

A simple power control algorithm for the radar replies, based on an AWGN model of the wireless channel, is presented. The radar interrogates aircraft transponders which respond with aircraft information using a directional antenna. For bidirectional communication between aircraft i and radar j, the received power $y_{ij}(t)$ at time t is

$$y_{ij}(t) = p_i(t) + c_{ij}(t),$$

where $p_i(t)$ is the reply transmit power of aircraft i and $c_{ij}(t)$ is the channel attenuation from aircraft i to radar j at time t. The received transmission can be successfully detected only if $y_{ij}(t) \geq \nu$, otherwise it is in outage, where ν is a predefined threshold [34]. The minimum transmit power that avoids outage is given by $p_i(t) = \nu - c_{ij}(t)$. The channel attenuation $c_{ij}(t)$ at time t can be closely approximated by the attenuation of an interrogation from radar j to aircraft i at the previous time instant, $c_{ji}(t-1)$. The channel link gain matrix is expected to change slowly compared to the interval between interrogator and reply transmissions, i.e., $c_{ji}(t-1) \approx c_{ji}(t)$. In addition, assuming symmetric channel attenuation ($c_{ij}(t) \approx c_{ji}(t)$), aircraft i can approximate the channel attenuation of $c_{ij}(t)$ by $c_{ji}(t-1)$. A simple algorithm can then be derived to calculate $p_i(t)$:

$$p_i(t) = \nu - c_{ji}(t-1) + \varepsilon, \quad (2)$$

where ε is the offset considering fading. $\varepsilon = \sigma Q^{-1}(1 - P_s)$, where P_s denotes the required reply reception rate and the Q-function, $Q = 0.5(1 - \mathrm{erf}(1/\sqrt{2}))$ where erf is the standard error function. When each aircraft i receives an interrogation, it recalls the transmit power level of radar j and estimates the channel loss. It then replies with the transmit power $p_i(t)$ given by Eq. (2).

B. Channel Access Control

In order to satisfy the minimum separation constraint between two aircraft, the control strategy can tolerate a certain maximum amount of latency in the system. Therefore, each aircraft is required to have at least one successful broadcast within a maximum allowable SUI η_i, with a minimum probability Γ_i. Recall that the SUI is the time between its successful state vector reports. Section V describes how the value of η_i will be determined by the control strategy. Here, the channel access problem is first formulated as an optimization problem. Then, a simple distributed algorithm that achieves globally optimal update rates using only local information is proposed. The constraint on the SUI can be described by

$$\Pr\left[\mu_i(\boldsymbol{\tau}) \leq \eta_i\right] \geq \Gamma_i\,, \quad \forall i \in N, \quad (3)$$

where τ_i is the channel access probability of aircraft i, $\boldsymbol{\tau}$ is the corresponding vector, N denotes the set of aircraft, μ_i is the SUI of aircraft i (a function of the vector $\boldsymbol{\tau}$), η_i is the desired maximum allowable SUI and Γ_i is the lower bound on the probability with which the SUI is less than η_i.

Let us assume that aircraft i is sampled with a period h_i and that the probability of a successful broadcast is $\gamma_i(\boldsymbol{\tau})$. Packet loss is modeled as a Bernoulli random process with parameter $1 - \gamma_i(\boldsymbol{\tau})$. Assuming $\eta_i \gg h_i$, the number of transmissions is approximately $\frac{\eta_i}{h_i}$ in time η_i Therefore, Eq. (3) becomes

$$1 - \left(1 - \gamma_i(\boldsymbol{\tau})\right)^{\frac{\eta_i}{h_i}} \geq \Gamma_i\,, \quad \forall i \in N. \quad (4)$$

The SUI constraint is interpreted as a delivery ratio requirement. After some manipulation, Eq. (4) can be written as

$$\gamma_i \geq \gamma_{i,\min} \triangleq 1 - \exp\left(\frac{h_i}{\eta_i} \log(1 - \Gamma_i)\right), \quad (5)$$

where $\gamma_{i,\min}$ is the minimum required probability of successful broadcast of aircraft i for distributed control. The control designer has the flexibility to tune the parameters η_i and Γ_i. Note that $\gamma_{i,\min}$ increases as the maximum allowable SUI decreases. This means that there is less slack in the network requirements when fast control is desired. Eq. (5) captures the interaction between the communication and control components.

The probability to meet the SUI requirement in Eq. (4) is an increasing function in $\gamma_i(\boldsymbol{\tau})$. Therefore, we address the problem of how each aircraft should decide its channel access probability to maximize broadcast throughput. By considering

the network utility maximization problem with weight factors [36], the channel access probability vector $\boldsymbol{\tau}^* = (\tau_i^*, i \in N)$, that maximizes network broadcast throughput is given by

$$\boldsymbol{\tau}^* = \arg \max_{0 \le \tau_i \le 1} \sum_{i \in N} -\gamma_{i,\min} \log \gamma_i(\boldsymbol{\tau}), \quad (6)$$

where $\gamma_{i,\min}$ is given in Eq. (5). The objective function of Eq. (6) assigns more network resources as $\gamma_{i,\min}$ increases i.e., more network resources for faster control systems. Different utility functions are discussed in [36].

The probability of successful broadcast $\gamma_i(\boldsymbol{\tau})$ is now derived in the context of random access networks. Consider a general wireless network, where all aircraft need not be within transmission range of each other. The network is modeled as an undirected graph. A link exists between two aircraft if and only if they can receive each other's transmissions.

***Proposition** 1:* The probability of a successful broadcast by aircraft i is

$$\gamma_i(\boldsymbol{\tau}) = \tau_i \prod_{j \in O_i} (1 - \tau_j) \prod_{k \in S_i} (1 - \tau_k), \quad \boldsymbol{\tau} \in \boldsymbol{\tau}_F, \quad (7)$$

where τ_i is the channel access probability of aircraft i, $\boldsymbol{\tau}$ denotes the vector of channel access probabilities for all aircraft, $\boldsymbol{\tau}_F$ is the feasible region for $\boldsymbol{\tau}$, i.e., $\boldsymbol{\tau}_F = \boldsymbol{\tau} : 0 \le \tau_i \le 1, \forall i \in N$, O_i represents the set of aircraft that can receive i's signals, and S_i denotes the set of the neighbors' neighbors of aircraft i.

Proof: The transmission of a given aircraft is successful if the following holds: (1) the destination aircraft is not transmitting, and (2) the other neighbors of the destination aircraft are not transmitting. In each slot, each aircraft i transmits a packet with probability τ_i. For any aircraft i, the set of i's neighbors, $O_i = \{j : (i,j) \in E\}$, represents the set of aircraft that can receive i's signals. The set of two-hop neighbors of i, $S_i = \cup_{j \in O_i} O_j \setminus \{O_i \cup \{i\}\}$, represents the set of neighbors that can receive j's signals for $j \in O_i$, excluding O_i and i. A broadcast from aircraft i is successful if and only if no aircraft in $O_i \cup S_i$ transmits during the same slot. The probability of a successful broadcast from aircraft i is given by Eq. (7). The term $\prod_{j \in O_i}(1 - \tau_j) \prod_{k \in S_i}(1 - \tau_k)$ is the probability that a packet transmitted from aircraft i is successfully received by neighbors $j \in O_i$. Note that $\prod_{j \in O_i}(1 - \tau_j)$ means that an aircraft is not allowed to transmit and receive simultaneously, and $\prod_{k \in S_i}(1 - \tau_k)$ means that an aircraft cannot receive from more than one neighbor at the same time. ■

A distributed algorithm that uses Eq. (7) to achieve the optimal channel access probability is now described.

***Theorem** 1:* The optimal access probability of aircraft i is given by

$$\tau_i^* = \frac{\gamma_{i,\min}}{\gamma_{i,\min} + \sum_{j \in L_i} \gamma_{j,\min}}, \quad (8)$$

where L_i is the set of aircraft that are one-hop or two-hop neighbors of aircraft i and $\gamma_{i,\min}$ is given by Eq. (5).

Proof: The objective function of Eq. (6) is written as

$$U(\boldsymbol{\tau}) = -\sum_{i \in N} \gamma_{i,\min} \left(\log \tau_i + \sum_{j \in L_i} \log(1 - \tau_j) \right),$$

where $L_i = O_i \cup S_i$ denotes the set of aircraft that are one-hop or two-hop neighbors of aircraft i. The function $\log \tau_i$ is concave in τ_i. For $i \in N$, $\sum_{j \in L_i} \log(1 - \tau_j)$ is thus a concave function of τ_j. Therefore, $U(\boldsymbol{\tau})$ is a concave function of $\boldsymbol{\tau}$. $U(\boldsymbol{\tau})$ has a unique global maximum by $\boldsymbol{\tau}^* = (\tau_i^*, i \in N)$, where $\nabla U(\boldsymbol{\tau})|\boldsymbol{\tau}_* = 0$. After some manipulation, the optimal access probability can be shown to be given by Eq. (8). ■

The optimal access probability τ_i^* of aircraft i satisfies the constraints $0 \le \tau_i^* \le 1$. Each aircraft computes its optimal access probabilities if it has information about its neighbors as well as the neighbors' neighbors. When the network is formed, or the network topology changes due to the joining, leaving or movement of aircraft, each aircraft broadcasts the information of its neighbors to all aircraft within its transmission range. This algorithm is implemented in a distributed manner with a small amount of local information exchange.

V. Control Strategy

Current air traffic control procedures compartmentalize sections of the airspace in order to minimize the workload of the human controllers. While this ensures the safe transit of all aircraft through the airspace, uncoordinated handoffs from one sector to the next frequently result in congestion in near the airport. This means that aircraft arrive almost unimpeded into the vicinity of the airport, but then spend a large amount of time orbiting in holding patterns while waiting for landing clearance. A high number of aircraft in a relatively small volume of airspace is a safety hazard, and also results in high fuel consumption because the aircraft have to fly longer at low altitudes. Thus there is a significant performance loss associated with current protocols.

In this paper, we propose a control algorithm to minimize the flight times of aircraft from the time of appearance at the periphery of the airspace around an airport, to their eventual landing at the airport. The primary control variable in this formulation is a change in velocity. A minimum separation requirement between each pair of aircraft is imposed for safety. Trajectory modifications (holding patterns) are avoided as far as possible in order to maximize safety [37]. An aircraft is sent to a holding pattern (an elliptical trajectory designed to introduce separation between aircraft) only if no feasible velocity is found to resolve a projected conflict. The proposed control algorithm can either be automatically implemented by the aircraft involved in a potential conflict, or provide conflict resolution advisories to the pilot and the controllers.

The relative geometry between a given pair of aircraft depends on the links that they currently occupy. Broadly, any two links in the network of Fig. 1 can be classified as being *paired* or *unpaired*. Two links are said to be paired if they lead to the same fix, otherwise they are said to be unpaired. This distinction is important when considering the separation requirement between aircraft. If two aircraft are on paired links, the point of closest approach between them may occur before the merge point. In the next section, a geometrical constraint on the velocity of the trailing aircraft in a paired merge is derived.

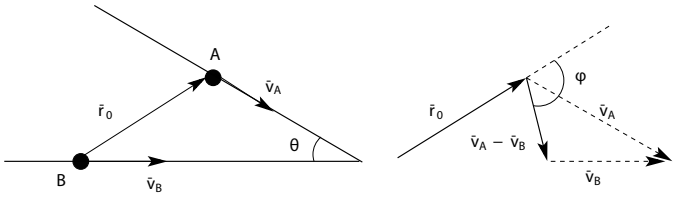

Fig. 2: Geometry for calculating the distance of closest approach.

A. Velocity Constraint for Paired Merges

Consider the geometrical layout shown in Fig. 2. Let the relative position of aircraft A with respect to B at the instant of initial contact be $\bar{r}_0$, their respective velocity vectors be $\bar{v}_A$ and $\bar{v}_B$, and the merge angle be θ. Let the relative velocity be given by $\bar{v}_r = \bar{v}_A - \bar{v}_B$ and the angle between $\bar{r}_0$ and $\bar{v}_r$ by ϕ. Then the distance and time of closest approach between A and B can be calculated using the relations derived in [38]. The time of closest approach is given by

$$t_c = -\left(\frac{\bar{r}_0 \cdot \bar{v}_r}{\bar{v}_r \cdot \bar{v}_r}\right),$$

and the relative position at the instant of closest approach is

$$\bar{r}_c = \bar{r}_0 + \bar{v}_r\, t_c = \bar{r}_0 - \bar{v}_r \left(\frac{\bar{r}_0 \cdot \bar{v}_r}{\bar{v}_r \cdot \bar{v}_r}\right).$$

The magnitude of the distance of closest approach is given by

$$r_c^2 = \bar{r}_c \cdot \bar{r}_c = r_0^2\, \sin^2\!\phi.$$

Let the minimum separation required between two aircraft at any time be $s_{\min}$. Therefore, the maximum allowable value of ϕ is given by

$$r_0^2\, \sin^2\!\phi = s_{\min}^2 \quad \Rightarrow \quad \sin\phi = \frac{s_{\min}}{r_0}. \tag{9}$$

The initial distance between A and B should be more than $s_{\min}$ for this relation to be valid. The value of ϕ decreases monotonically after initial contact, and the point of closest approach is reached when $\phi = \frac{\pi}{2}$. Therefore, if the initial value of ϕ is less than $\frac{\pi}{2}$, the distance between A and B increases monotonically. To maximize v_B while still maintaining separation, it should satisfy Eq. (9) with $\phi > \frac{\pi}{2}$. Finally, this constraint is not active if $\phi < \frac{\pi}{2}$, or if the projected point of closest approach is beyond the merge point. Note that the geometric constraint is valid for the three-dimensional case as well, but is more difficult to visualize. In addition, most merges in actual airspace do not occur while aircraft are changing altitude. Therefore, it is reasonable to consider only two-dimensional merging scenarios.

B. Optimal Velocities for Paired Merges

Suppose the aircraft A and B are at a distance s_A and s_B respectively from the merge point in Fig. 2. The optimal velocities v_A and v_B that minimize the time at which the trailing aircraft B reaches the merge point are given by:

$$\begin{aligned} \min_{v_A, v_B} \quad & \frac{s_B}{v_B} && (10)\\ \text{s.t.} \quad & v_A \le v_{A,\max}, \quad v_B \ge v_{B,\min} && \text{(Feasibility)}\\ & v_B \le f(v_A, s_A, s_B). && \text{(Separation)} \end{aligned}$$

Here, f is the constraint on v_B as explained in Section V-A, active when the aircraft are in danger of breaching the minimum separation requirement. Optimal values of v_A and v_B can be calculated using Lagrange multipliers, and are given by $v_A = v_{A,\max}$, with v_B satisfying the separation constraint with equality. The optimal value for v_B can be calculated numerically in a very short time, since it is the result of a one-dimensional search with a known minimum constraint $v_{B,\min}$.

C. Synthesized Control Strategy

The central facility calculates velocities for all aircraft in the centralized zone by estimating the current state of the airspace, based on the last known location and velocity of each aircraft. Expected landing times are calculated for each aircraft, thus generating a priority order for the centralized zone. Conflict detection is carried in a pairwise fashion for each pair of aircraft, starting with the aircraft that has the highest priority. Resolution maneuvers (if required) are commanded for the aircraft that are lower in the priority order. Consequently, an aircraft that is i^{th} in the priority order for landing could have up to $(i-1)$ downward adjustments of its commanded velocity while the control algorithm is processing data. If the commanded velocity is less than the least feasible velocity for that aircraft, it is commanded to enter a holding pattern. Once the computation is completed, the final velocity commands are transmitted to each aircraft. Calculating optimal velocities for all aircraft in the centralized zone only requires a few hundredths of a second in terms of computation time, since it is a repeated application of the pairwise calculations from Section V-B. The necessity of commanding holding patterns is a function of the traffic demand, as explained in Section VI-B.

If successive aircraft are on paired links, the values are calculated using the relations described in Section V-B. If they are on unpaired links, the algorithm allows for the minimum separation of $s_{\min}$ at their projected merge point. If two successive aircraft are on the same link, a separation of $s_{\min}$ is ensured at all times, subject to the physical velocity constraints of each aircraft. If no feasible velocity is found for an aircraft, it is sent to a holding pattern, and resumes its original trajectory after a period of 2 min. This value is a realistic estimate of the time required to complete holding patterns in actual flight. Finally, optimal velocities are recalculated based on two trigger events: the entry of a new aircraft into the zone of centralized control, or the start or end of a holding pattern by at least one aircraft. The rest of the time, the central facility operates in passive monitoring mode.

Outside the centralized zone, the control algorithm uses local information received from ADS-B transmissions. In this paper, each ADS-B message is assumed to include a time stamp, and the maximum and minimum achievable velocities of the aircraft. Suppose aircraft A outside the centralized zone receives a transmission from aircraft B for the first time. It first decides on a pairwise order based on the projected arrival times of both aircraft at their eventual merge point. If aircraft A projects itself as arriving before B at the merge point, it only notes the presence of B but does not adjust its velocity. If it projects that aircraft B will arrive at the merge point first, it

computes a new velocity for itself in order to not conflict with B, while still flying as fast as possible. If B is also outside the centralized zone, it carries out a complementary set of calculations on detecting A for the first time. Even if aircraft B is under centralized control, it does not affect the computations carried out by aircraft A. Finally, in addition to the detection of a new aircraft, an aircraft recalculates its velocity if there is a change in state (link, velocity or hold) of another aircraft already being tracked. Since each pair of aircraft decides on a mutual order at the merge point, a unique ordering of all aircraft heading to a given merge point is developed.

D. Challenges for Control Implementation

There are several issues to overcome before the proposed algorithm can be implemented in practice. Firstly, due to stochastic transmission times and possible packet loss, state updates between an aircraft and another aircraft or the central facility are asynchronous. However, the time stamp within each ADS-B message allows the estimation of the current state of each aircraft, and also reduces the likelihood of inconsistent calculations in the distributed algorithm. Additionally, it guards against a mismatch caused by the clocks on two aircraft not being synchronized. As long as all aircraft use the transmitted time stamps, computations will be consistent.

Uncertainty, both in state measurement and in velocity, is also a challenge to practical implementation. The proposed algorithm can account for uncertainty by appropriately buffering the minimum separation constraint. Finally, there is a non-zero probability that two aircraft are projected to reach their merge point at exactly the same time. In this case, the asynchronous nature of ADS-B transmissions proves beneficial. The distributed control algorithm is set to give precedence to the other aircraft in case of deadlock. Since it is very likely that one aircraft receives a state update before the other, it will already have slowed down by the time the other aircraft begins its computations. Even if message delivery is nearly simultaneous and both aircraft reduce their own velocities, a small time difference between the adjustments will be sufficient to resolve the deadlock in the next computation cycle.

The control algorithm also gives precedence to non-cooperative aircraft in the airspace, which could be present because of a lack of ADS-B equipage, equipment failure, or some other onboard emergency. Actual non-cooperative behavior can be differentiated from message reception failure by using the SUI to calculate the probability of no messages being received by the aircraft in a given time window. The SUI is important from the point of view of stability of the control algorithm, for example, if an aircraft has to slow down suddenly. Recall that the SUI is used to design the channel access control of the communication protocol in Section IV.

The maximum allowable SUI that retains network stability is derived below. It is assumed that aircraft arriving earlier at the merge point have higher priority, and that they can change their velocities without considering the aircraft behind them. Suppose aircraft A, flying at velocity v_A, and B, flying at v_B (Fig. 2) have previously made contact while at distances s_A and s_B from the merge point, and aircraft A has priority.

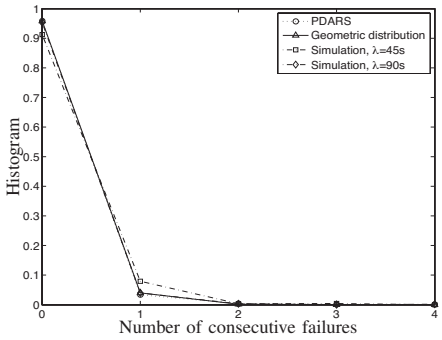

Fig. 3: Histogram of the number of consecutive failures of the radar sweep obtained by PDARS data, approximated geometric distribution, and simulation results.

Aircraft A now reduces its velocity to $v'_A \leq v_A$ while at a distance d_A from the merge point. Aircraft B, which is at distance d_B from the merge point, needs to adjust its own velocity to maintain separation with aircraft A. Nominally, aircraft A would reach the merge point after a further time $t_A = \frac{d_A}{v_A}$, which is changed to $t'_A = \frac{d_A}{v'_A} \geq t_A$. The instant of closest approach can be approximated by assuming that aircraft B is going to be in conflict with aircraft A at a time $(t'_A - t_A)$ before aircraft A arrives at the merge point. η_A denotes the maximum allowable SUI after which aircraft B can receive an update from aircraft A, and still not have to enter a holding pattern. In other words, aircraft B flies at its original velocity for a further time η_A, after which it slows to $v_{B,\min}$ until aircraft A is at the merge point. At this time, aircraft B needs to be at a distance $s_{\min}$ from it. Equating the distance covered by aircraft B up to time t_A in the nominal case and up to time t'_A under the actual case, yields:

$$d_B - s_{\min} = \underbrace{v_B\,\eta_A + v_{B,\min}\left(\frac{d_A}{v'_A} - \eta_A\right)}_{\text{Actual scenario}} = \underbrace{v_B\,\frac{d_A}{v_A}}_{\text{Original scenario}}.$$

Simplifying the above equation, the maximum allowable SUI for communication from aircraft A to aircraft B is

$$\eta_A = \frac{\frac{d_A}{v_A}\,v_B - \frac{d_A}{v'_A}\,v_{B,\min}}{v_B - v_{B,\min}}. \tag{11}$$

Eq. (11) suggests that as d_A decreases, that is, as aircraft A approaches the merge point, it needs faster updates in case of velocity changes. If aircraft B is already flying at its minimum speed ($v_B = v_{B,\min}$), then $v'_A = v_A$, that is, aircraft A cannot slow down without causing aircraft B to change its trajectory to maintain separation. In the nominal case, $v_A = v'_A$ and Eq. (11) implies $\eta_A = \frac{d_A}{v_A}$. Aircraft A only needs to transmit an update when it reaches the merge point, supporting the assumption that control computations need only be run when aircraft transition from one link to another. For any $v'_A < v_A$, the maximum allowable SUI is less than $\frac{d_A}{v_A}$, that is, there must be an update before aircraft A arrives at the intersection. Note that the maximum allowable SUI is the essential requirement to guarantee the safety for maintaining the minimum separation requirement between aircraft. The maximum allowable SUI is used to optimize the performance of communication protocols in Section IV-B.

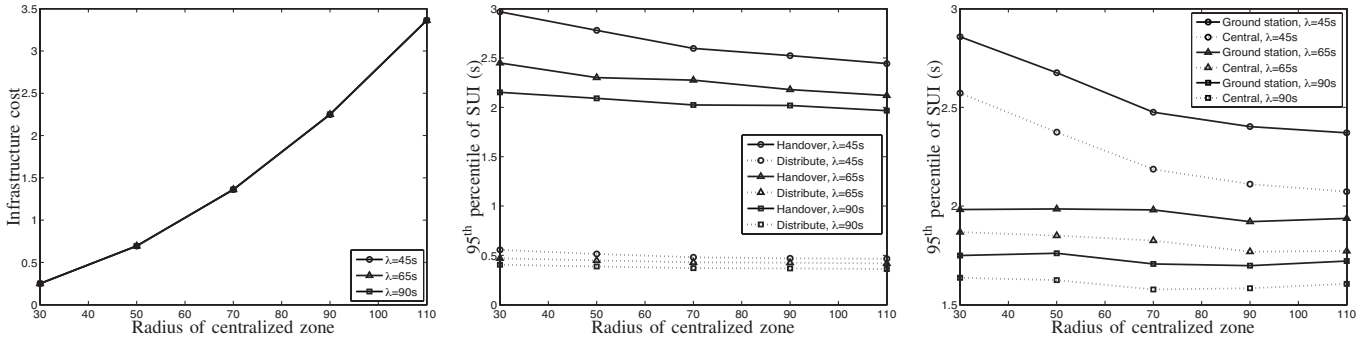

(a) Infrastructure cost. (b) ADS-B SUI. (c) Centralized SUI.

Fig. 4: Infrastructure cost, ADS-B SUI, and centralized SUI as a function of the radius of centralized zone for different traffic loads. Note that the level of confidence is represented as a percentile.

VI. Performance Evaluation

The performance of the proposed hybrid communication and control strategy is evaluated in this section. The simulations are carried out using a realistic model of air traffic operations into LAX in Fig 1. We develop a simulation environment comprehensively modeling the complex interplay among the air traffic load, the ground radar systems, the ADS-B systems, and the wireless channel [5]. The simulation model consists of three main components: the air traffic model, the surveillance network model, and the wireless channel model. Our simulator provides statistics on the wireless link performance and tracking information of a flight based on a realistic airspace model. Individual flights are simulated from their initial appearance $600\,\mathrm{nm}$ from the airport, until their arrival at the airport. The arrival trajectories are derived from the published standard terminal arrival routes for LAX, and verified using data from the FAA's Performance Data Analysis and Reporting System (PDARS). The simulation framework contains a communication model that captures SINR-based signal propagation [35]. Although departing aircraft are separated by altitude, they are significant from a communication perspective, and are therefore included in the simulation. Consistent with ADS-B standards [3], the range of the transmit power and the required threshold to receive a packet are set to is $51-57$ dBm and -84 dBm, respectively.

LAX carried out 703,000 total operations in 2011 [39], which translates to 963 arrivals per day on average, or one aircraft every 90 s. Since current operations consist of demand peaks and lulls, the daily average is a good approximation to the average arrival rate seen over several hours. The uncertain nature of demand is captured by the assumption that aircraft appear at the boundary of the simulated region as a Poisson process with average inter-arrival time $\lambda = 90\,\mathrm{s}$. To account for future traffic levels, 1.5 times ($\lambda = 65\,\mathrm{s}$) and 2 times the current traffic level ($\lambda = 45\,\mathrm{s}$) are also simulated.

A. Communication Performance

The simulation results are validated through comparisons with the PDARS (actual radar measurements from the Southern California sector). Fig. 3 shows a histogram of the number of consecutive failures of the radar sweep (as measured by missed target hits in the PDARS data), the approximated geometric distribution, and simulation results corresponding to traffic loads $\lambda = 45\,\mathrm{s}$ and $90\,\mathrm{s}$. The distribution of the consecutive radar sweep failures matches well with both a geometric model and simulations for the current traffic load, $\lambda = 90\,\mathrm{s}$. It can therefore be assumed that the burst length of a wireless link is small enough to make a time-independence assumption for that link. Since ADS-B was not operational at the time of the PDARS measurements, they reflect radar performance without interference from ADS-B. As the number of aircraft increases ($\lambda = 45\,\mathrm{s}$), the failure probability increases due to increased interference from ADS-B.

There is a fundamental tradeoff between infrastructure cost and SUI of the network. Fig. 4 shows the variation of the

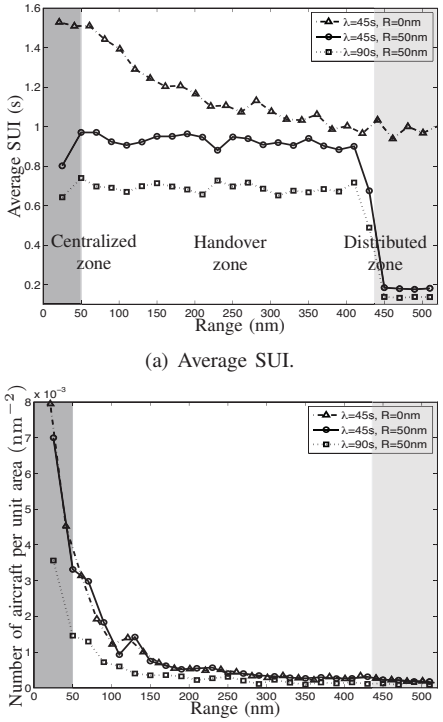

(a) Average SUI.

(b) Aircraft density.

Fig. 5: Average SUI and aircraft density as a function of the distance from the airport. The dark and light gray colored areas present the centralized and distributed zones, respectively. Note that $R = 0\,\mathrm{nm}$ refers to ADS-B systems with maximum transmit power and default number of transmissions.

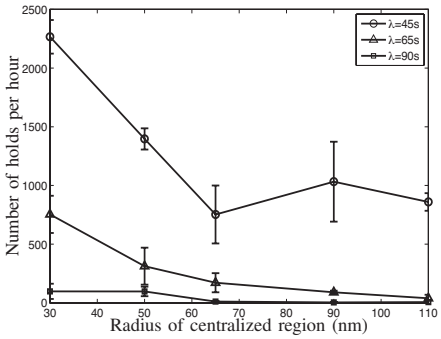

Fig. 6: Average number of holds as a function of the radius of centralized zone.

infrastructure cost (average cost of radars to cover the centralized zone), ADS-B SUI, and centralized SUI as a function of the radius of the centralized zone, for traffic loads $\lambda = 45\,\mathrm{s}$, $65\,\mathrm{s}$ and $90\,\mathrm{s}$. Note that the 95$^{\text{th}}$ percentile is set as the default level of confidence for computing the SUI. In Fig. 4(a), the cost is seen to increase monotonically with the radius of the centralized zone. Fig. 4(b) compares the 95$^{\text{th}}$ percentile of the ADS-B SUI for the handover and distributed zones as a function of the radius of the centralized zone. Note that the performance of the SUI is essential to guarantee the minimum separation requirement between aircraft as described in Section V-D. Outside the centralized zone, a track update is considered completed when an ADS-B broadcast is successful, that is, it is successfully received by all receivers located in the local broadcasting region. The gains in efficiency across different traffic loads for the distributed zone are found to be small compared to those in the handover zone, due to the larger distance from the centralized zone. Fig. 4(c) shows the 95$^{\text{th}}$ percentile of the SUI of ADS-B ground stations and the SUI for the centralized zone. The SUI of the centralized zone combines the state update of aircraft by using ADS-B ground stations and ground radar systems. The SUI of the centralized zone increase as the radius of centralized zone decreases, especially when the traffic load is high ($\lambda = 45\,\mathrm{s}$). This is due to the increase in interference from ADS-B as the radius of the centralized zone decreases, since each aircraft only reduces its transmit power and channel access probability close to the centralized zone as described in Section IV. Although the SUI depends on the radius of the centralized zone, a lower traffic load has a lower SUI than higher traffic loads due to lower interference levels.

Finally, Fig. 5 shows the average SUI and number of aircraft per unit area as a function of the distance from the airport, for different traffic loads $\lambda = 45\,\mathrm{s}$ and $90\,\mathrm{s}$, and radii of centralized zone $R = 0\,\mathrm{nm}$ and $50\,\mathrm{nm}$. Aircraft are grouped into $20\,\mathrm{nm}$ bins based on their distance from the airport. The dark and light gray colored areas represent the centralized and the fully distributed zones of the communication protocol, respectively. $R = 0\,\mathrm{nm}$ refers to ADS-B systems with maximum transmit power and default number of transmissions. The average SUI changes with distance from the airport due to the variation in ground radar and aircraft densities. The number of aircraft in the terminal area is larger than elsewhere in the airspace. The average SUI is large for an aircraft in the terminal area because

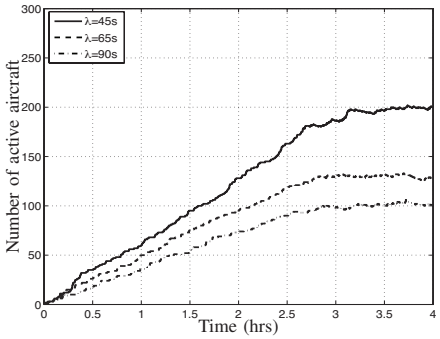

(a) Radius of centralized region = $110\,\mathrm{nm}$

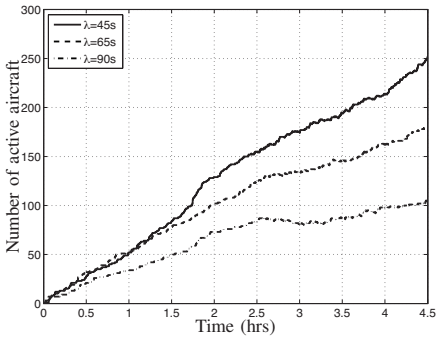

(b) Radius of centralized region = $30\,\mathrm{nm}$

Fig. 7: Number of active aircraft in the airspace based on different traffic loads and different sizes of the centralized region.

the interrogation rate and aircraft density are both high, leading to significant interference. For $R = 0\,\mathrm{nm}$, the average SUI increases significantly close to the airport due to the use of maximum transmit power. For the other cases, transmit power and channel access probability are minimized within the centralized zone to reduce interference with radars. Distributed access control is seen to significantly reduce the average SUI outside the centralized zone, illustrating the effectiveness of the proposed solution.

B. Control Performance

Holding patterns in the airspace are an indicator of congestion and instability within the network. These holds are necessary when just a velocity change by an aircraft cannot guarantee safety. In dense traffic, one holding pattern typically causes a cascade of holding patterns upstream, affecting a large section of the airspace. Fig. 6 shows the average number of holds commanded per hour for traffic loads $\lambda = 45\,\mathrm{s}$, $65\,\mathrm{s}$ and $90\,\mathrm{s}$, as a function of the radius of the centralized region. The benefits of moving from a radius of $65\,\mathrm{nm}$ to $110\,\mathrm{nm}$ are seen to be quite small. As the traffic arrival rate increases, there are large benefits in moving from a $30\,\mathrm{nm}$ radius to a $65\,\mathrm{nm}$ radius. This trend is similar to the one seen for communication performance in Fig. 4.

Fig. 7 further emphasizes the unstable nature of the network for high traffic rates and small centralized zones. It shows a time series of traffic for two different sizes of the centralized zone. Centralized control applied to the larger region ($R = 110\,\mathrm{nm}$) is seen to stabilize the traffic in all three cases $\lambda = 45,\ 65,\ 90\,\mathrm{s}$. On the other hand, the smaller

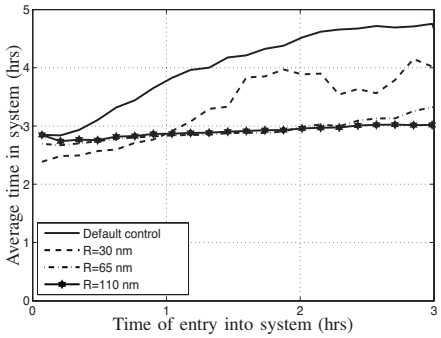

Fig. 8: Performance comparison of the default control algorithm and the proposed control algorithm.

region ($R = 30\,\mathrm{nm}$) cannot cope with higher traffic loads, and experiences a continuous increase in the number of active aircraft in the airspace, most of which have been delayed in the central region. While holding patterns are generated in bursts, low to moderate traffic loads allow the airspace to recover and resume smooth operations. However, traffic accumulates if more holds are generated before this recovery is complete, as can happen with high traffic loads.

Current air traffic control procedures rely heavily on human supervision, and are difficult to model exactly. However, it is reasonable to assume that aircraft are only deconflicted up to the next merge point, and downstream conflicts are resolved as they emerge. Fig. 8 compares this approach to the proposed control strategy for $\lambda = 65\,\mathrm{s}$. It shows the average amount of time required by aircraft at the periphery to land at the airport. Since all the simulations start with an empty airspace model, the initial flight times for all cases are similar (approximately 2.75 hours). However, as time progresses and the airspace congestion increases, the difference in performance becomes significant. The proposed control algorithm performs significantly better than the current operations for all values of the central radius. Increasing the radius of the centralized region increases the efficiency of the control algorithm up to a point (seen to be at $65\,\mathrm{nm}$ for the current model), beyond which the marginal benefits are minimal.

Decreasing the radius of the centralized zone reduces the number of ground radars near a terminal area and the associated ground infrastructure cost, as shown in Fig. 4(a). However, a smaller centralized zone degrades both communication (Figs. 4(b) and 4(c)) and control performance (Fig. 6). An arbitrarily large region of centralized control not only entails large costs, but also fails to show significant improvement in performance. The traffic density far away from an airport is small enough for the distributed control algorithm to perform nearly as good as the centralized algorithm.

VII. Conclusions

This paper presents a framework combining communication and control to improve the safety and efficiency of NextGen. Issues governing the level of decentralization are analyzed, and it is shown that the introduction of ADS-B improves overall system performance. The performance of the proposed algorithm is evaluated through simulations on a realistic air traffic system model, and validated using actual surveillance data. The practical challenges associated with control over an imperfect communication link are investigated. Numerical results show that the proposed scheme significantly improves the performance of the communication, navigation, and surveillance systems under increasing traffic levels. The proposed hybrid centralized/distributed strategy has performance comparable to fully centralized strategies, while requiring significantly less ground infrastructure. The tradeoffs between infrastructure cost and system performance depending on the level of decentralization are also discussed.

Future work will include the stability analysis of the distributed control algorithm using queueing theory. Multihop communication protocols will also be developed to manage congestion in the distributed zones.

References

[1] *NextGen Implementation Plan*, FAA, 2011, http://www.faa.gov/nextgen/media/NextGen_Implementation_Plan_2011.pdf.
[2] E. A. Lester and R. J. Hansman, "Benefits and Incentives for ADS-B Equipage in the National Airspace System," MIT, Tech. Rep., 2007.
[3] *Minimum Aviation System Performance Standard for Automatic Dependent Surveillance Broadcast (ADS-B)*, RTCA, 2002, DO-242A.
[4] K. Sampigethaya, R. Poovendran, S. Shetty, T. Davis, and C. Royalty, "Future e-enabled aircraft communications and security: The next 20 years and beyond," *Proceedings of the IEEE*, vol. 99, no. 11, pp. 2040–2055, 2011.
[5] P. Park and C. Tomlin, "Investigating communication infrastructure of next generation air traffic management," in *ACM/IEEE ICCPS*, 2012.
[6] J. K. Kuchar and L. C. Yang, "A review of conflict detection and resolution modeling methods," *IEEE Transactions on Intelligent Transportation Systems*, vol. 1, no. 4, pp. 179–189, 2000.
[7] G. Miao, N. Himayat, G. Li, and S. Talwar, "Distributed interference-aware energy-efficient power optimization," *IEEE Transactions on Wireless Communications*, vol. 10, no. 4, pp. 1323–1333, 2011.
[8] S. Kucera, S. Aissa, K. Yamamoto, and S. Yoshida, "Asynchronous distributed power and rate control in ad hoc networks: a game-theoretic approach," *IEEE Transactions on Wireless Communications*, vol. 7, no. 7, pp. 2536–2548, 2008.
[9] J. Wieselthier, G. Nguyen, and A. Ephremides, "On the construction of energy-efficient broadcast and multicast trees in wireless networks," in *IEEE INFOCOM*, 2000.
[10] A. Ephremides and T. Truong, "Scheduling broadcasts in multihop radio networks," *IEEE Transactions on Communications*, vol. 38, no. 4, pp. 456–460, 1990.
[11] I. Chlamtac and S. Kutten, "On broadcasting in radio networks–problem analysis and protocol design," *IEEE Transactions on Communications*, vol. 33, no. 12, pp. 1240–1246, 1985.
[12] I. Rhee, A. Warrier, J. Min, and L. Xu, "DRAND: Distributed randomized TDMA scheduling for wireless ad hoc networks," *IEEE Transactions on Mobile Computing*, vol. 8, no. 10, pp. 1384–1396, 2009.
[13] R. Rom and M. Sidi, *Multiple access protocols: performance and analysis*. Springer-Verlag, 1990.
[14] A. Banchs, P. Serrano, and H. Oliver, "Proportional fair throughput allocation in multirate IEEE 802.11e wireless LANs," *Wireless Networks*, vol. 13, pp. 649–662, 2007.
[15] Y. Jian, M. Zhang, and S. Chen, "Achieving mac-layer fairness in csma/ca networks," *IEEE/ACM Transactions on Networking*, vol. 19, no. 5, pp. 1472–1484, 2011.
[16] A. Raniwala, D. Pradipta, and S. Sharma, "End-to-End Flow Fairness Over IEEE 802.11-Based Wireless Mesh Networks," in *IEEE INFOCOM*, 2007.
[17] S. Chen, Y. Fang, and Y. Xia, "Lexicographic maxmin fairness for data collection in wireless sensor networks," *IEEE Transactions on Mobile Computing*, vol. 6, no. 7, pp. 762–776, 2007.
[18] "Free flight implementation," Task Force 3, RTCA Inc., Tech. Rep., 1995.
[19] J. Kovsecká, C. Tomlin, G. Pappas, and S. Sastry, "Generation of conflict resolution maneuvers for air traffic management," in *IEEE/RSJ IROS*, 1997.
[20] P. K. Menon, G. D. Sweriduk, and B. Sridhar, "Optimal strategies for free-flight air traffic conflict resolution," *Journal of Guidance, Control and Dynamics*, vol. 22, no. 2, pp. 202–211, 1999.

[21] A. Bicchi and L. Pallottino, "On optimal cooperative conflict resolution for air traffic management systems," *IEEE Transactions on Intelligent Transportation Systems*, vol. 1, no. 4, pp. 221–232, 2000.
[22] J. Hu, M. Prandini, A. Nilim, and S. Sastry, "Optimal coordinated maneuvers for three dimensional aircraft conflict resolution," *Journal of Guidance, Control and Dynamics*, vol. 25, no. 5, pp. 888–900, 2002.
[23] L. Pallottino, E. M. Feron, and A. Bicchi, "Conflict resolution problems for air traffic management systems solved with mixed integer programming," *IEEE Transactions on Intelligent Transportation Systems*, vol. 3, no. 1, pp. 3–11, 2002.
[24] C. E. van Daalen and T. Jones, "Fast conflict detection using probability flow," *Automatica*, vol. 45, no. 8, pp. 1903–1909, 2009.
[25] C. Tomlin, G. Pappas, and S. Sastry, "Conflict resolution for air traffic management: A study in multiagent hybrid systems," *IEEE Transactions on Automatic Control*, vol. 43, no. 4, pp. 509–521, 1998.
[26] Z.-H. Mao, E. Feron, and K. Bilimoria, "Stability and performance of intersecting aircraft flows under decentralized conflict avoidance rules," *IEEE Transactions on Intelligent Transportation Systems*, vol. 2, no. 2, pp. 101–109, 2001.
[27] H. Erzberger and K. Heere, "Algorithm and operational concept for resolving short-range conflicts," *Proceedings of the Institution of Mechanical Engineers, Part G: Journal of Aerospace Engineering*, vol. 224, pp. 225–243, 2009.
[28] A. Alonso-Ayuso, L. F. Escudero, and F. J. Martin-Campo, "A mixed 0-1 nonlinear optimization model and algorithmic approach for the collision avoidance in ATM: velocity changes through a time horizon," *Computers & Operations Research*, vol. 39, no. 12, pp. 3136–3146, 2012.
[29] J. Kuchar and A. Drumm, "The traffic alert and collision avoidance system," *Lincoln Laboratory Journal*, vol. 16, no. 2, pp. 277–296, 2007.
[30] "Introduction to TCAS II version 7.1," Federal Aviation Administration, Tech. Rep., 2011.
[31] "Annex 10 - volume 4," International Civil Aviation Organization, Tech. Rep., 2007.
[32] F. Netjasov, A. Vidosavljevic, V. Tosic, and H. Blom, "Systematic validation of a mathematical model of ACAS operations for safety assessment purposes," in *USA/Europe ATM R&D Seminar*, 2011.
[33] M. Prandini, J. Lygeros, A. Nilim, and S. Sastry, "A probabilistic framework for aircraft conflict detection," in *AIAA GNCCG*, 1999.
[34] *Minimum Operational Performance Standards for Air Traffic Control Radar Beacon System/Mode Select (ATCRBS/Mode S) Airborne Equipment*, RTCA, 1999, DO-181B.
[35] A. Goldsmith, *Wireless Communications*. Cambridge University Press, 2005.
[36] M. Chiang, S. Low, A. Calderbank, and J. Doyle, "Layering as optimization decomposition: A mathematical theory of network architectures," *Proceedings of the IEEE*, vol. 95, no. 1, pp. 255–312, 2007.
[37] M. Lupu, E. Feron, and Z.-H. Mao, "Traffic complexity of intersecting flows of aircraft under variations of pilot preferences in maneuver choice," in *IEEE CDC*, 2010.
[38] J. Krozel and M. Peters, "Strategic conflict detection and resolution for free flight," in *IEEE CDC*, 1997.
[39] N. A. Airports Council International, "2011 North American (ACI-NA) Top 50 airports," http://aci-na.org/content/airport-traffic-reports [Accessed 09-August-2012].

Pangun Park received the M.S. and Ph.D. degrees in electrical engineering from the Royal Institute of Technology, Sweden, in 2007 and 2011, respectively. Since 2011, he has been working as a postdoctoral researcher in electrical engineering and computer science from the University of California, Berkeley. He received the best paper award at the IEEE International Conference on Mobile Ad-hoc and Sensor System of 2009. His research interests include cyber-physical systems, air traffic surveillance networks, and wireless sensor and actuator networks.

Harshad Khadilkar is a graduate student in the Department of Aeronautics and Astronautics at the Massachusetts Institute of Technology. He received his Bachelors degree in Aerospace Engineering from the Indian Institute of Technology, Bombay. His research interests include algorithms for optimizing air traffic operations, and stochastic estimation and control.

Hamsa Balakrishnan is an Associate Professor of Aeronautics and Astronautics at the Massachusetts Institute of Technology. She received a B.Tech in Aerospace Engineering from the Indian Institute of Technology, Madras in 2000 and a PhD in Aeronautics and Astronautics from Stanford University in 2006. Between May and December 2006, she was a researcher at the University of California, Santa Cruz and the NASA Ames Research Center. Her research interests address various aspects of air transportation systems, including algorithms for air traffic scheduling and routing, integrating weather forecasts into air traffic management and minimizing aviation-related emissions; air traffic surveillance algorithms; and mechanisms for the allocation of airport and airspace resources. She was a recipient of the NSF CAREER Award in 2008, the Kevin Corker Award for Best Paper of ATM-2011, and the AIAA Lawrence Sperry Award in 2012.

Claire Tomlin is a Professor of Electrical Engineering and Computer Sciences at Berkeley, where she holds the Charles A. Desoer in Engineering. She held the positions of Assistant, Associate, and Full Professor at Stanford from 1998-2007, and in 2005 joined Berkeley. She has been an Affiliate at LBL in the Life Sciences Division since January 2012. She received the Erlander Professorship of the Swedish Research Council in 2010, a MacArthur Fellowship in 2006, and the Eckman Award of the American Automatic Control Council in 2003. She works in hybrid systems and control, with applications to biology, robotics, and air traffic systems.